Multivariate time-scale bootstrap for testing the equality of selfsimilarity parameters

Charles-Gérard LUCAS[1], Herwig WENDT[2], Patrice ABRY[1], Gustavo DIDIER[3]

[1]CNRS, ENS de Lyon, Laboratoire de Physique, Lyon (FR), firstname.lastname@ens-lyon.fr,

[2]IRIT, Université de Toulouse, CNRS, UT3, Toulouse (FR), herwig.wendt@irit.fr

[3]Mathematics Department, Tulane University, New Orleans (USA), gdidier@tulane.edu

Supported by PhD Grant DGA/AID (no 01D20019023), ANR-18-CE45-0007 MUTATION

Résumé – La surveillance d'un système à partir de données multivariées enregistrées par un ensemble de capteurs implique souvent de compter combien de paramètres d'autosimilarité effectivement différents pilotent leurs dynamiques temporelles. En utilisant un modèle de mouvement brownien fractionnaire multivarié, des procédures d'estimations construites sur les valeurs propres de représentations en ondelettes et une technique de bootstrap par bloc dans le domaine temps-échelle, un test d'égalité entre paires triées de paramètres d'autosimilarité estimés est construit. La procédure permet, à partir d'une seule observation de taille finie des données, d'estimer la p-valeur et la puissance du test. Les performances de la procédure sont quantifiées au moyen de simulations Monte Carlo de grandes tailles, conduites sous différents scénarios.

Abstract – Monitoring one system from multivariate data collected on multiple sensors often entails counting how many actually different selfsimilarity parameters drive their temporal dynamics. Making use of a multivariate fractional Brownian motion model, of multivariate eigenwavelet estimations, and of a multivariate time-scale block bootstrap procedure, a test for equality between pairs of sorted estimated selfsimilarity parameters is devised. The procedure permits the estimation of the test p-value and power from a single finite-size data observation. Test performance are quantified from large size Monte Carlo simulations performed under several scenarios.

1 Introduction

Context. In real-world applications, the monitoring of one system by means of a collection of sensors entails counting the number of actually different selfsimilarity parameters that drive the temporal dynamics of the corresponding time series [1] as a proxy for assessing the number of independent components in data. Practically testing the equality amongst pairs of estimated selfsimilarity exponents from a single observation of multivariate data constitutes the crucial issue at the heart of this work.

Related works. Selfsimilarity and fractional Brownian motion (fBm) [2–4] have long been used to model scale-free dynamics in numerous and various real world applications, while most recent applications entail analyzing jointly multivariate times series [1]. In the last decade, multivariate selfsimilarity models, such as the operator fractional Brownian motion (ofBm) [5–7], and multivariate wavelet based estimation procedures (cf. [8–10]) were developed, usually yielding vectors of estimated selfsimilarity parameters, with same size as the number of components in data. This leaves unaddressed the estimation of the numbers of actually different such parameters, a crucial issue in many applications, such as the analysis of infraslow brain activity (cf. [11]). In earlier works, wavelet-domain block-bootstrap hypothesis procedures were proposed for testing whether all selfsimilarity exponents are equal [12, 13], as first preliminary step, or for performing pairwise equality tests for estimated selfsimilarity parameters [14], yet not satisfactorily reproducing the targeted significance level for situations where some pairs are equal while others are not.

Goals, contributions and outline. This work devises a time-scale block bootstrap procedure for testing pairwise equality in selfsimilarity parameters that can actually be applied to a single and finite-size observation of data. Elaborating on [14], its originality consists in constructing bootstrap test statistics that correctly reproduce the test significance level under all scenarios, i.e., both for a single cluster — all pairs follow the null hypothesis ($\mathcal{H}_0$: pairwise equality in selfsimilarity parameters) — and for different numbers of clusters and cluster sizes (where some unknown pairs depart from $\mathcal{H}_0$). Section 2 recalls the multivariate selfsimilarity model and the eigenwavelet estimation procedure. Section 3 describes the key contributions of the work : the test principle, the statistical properties of the test statistic and its modeling with folded-normal distributions, as well as the bootstrap procedure, permitting to compute the test, estimate the p-value and also the power. Section 4 reports a large-size set of Monte Carlo simulations, performed under different scenarios and sample sizes, using 6-variate fBm. It validates the relevance of the proposed modeling of the test statistic and quantifies the ability of the bootstrap procedure to reproduce the actual test performance. OfBm synthesis, selfsimilarity exponent estimation and test procedures are implemented by the authors and available at `https://github.com/charlesglucas/ofbm_tools`.

2 Multivariate selfsimilarity

Multivarite selfsimilarity model. It has recently been proposed that multivariate selfsimilarity in time series can be modeled by the *operator fractional Brownian motion* [7]. In the present work, we use a simplified version of that model that we refer to as multivariate fBm (M-fBm). It is defined from a set of M dependent fBm [4], each with possibly different selfsimilarity exponents $\underline{H} = (H_1, \ldots, H_M)$, $0 < H_1 \leq \ldots \leq H_M < 1$, and covariance matrix Σ_X, mixed linearly via a $M \times M$ real-valued and invertible mixing matrix W :

$$Y \triangleq \{Y_1^{\underline{H},\Sigma_X,W}(t), \ldots, Y_M^{\underline{H},\Sigma_X,W}(t)\}_{t\in\mathbb{R}} \triangleq W\,\{X_{H_1}(t), \ldots, X_{H_M}(t)\}_{t\in\mathbb{R}} = WX. \quad (1)$$

Multivariate selfsimilarity parameter estimation. To estimate the vector of selfsimilarity paramaters $\underline{H}$, a procedure was devised in [9, 10], based on multivariate discrete wavelet transform coefficients $D_{Y_m}(2^j, k) = \langle 2^{-j/2}\psi_0(2^{-j}t - k)|Y_m(t)\rangle$, $\forall k \in \mathbb{Z}$, $\forall j \in \{j_1, \ldots, j_2\}$ with ψ_0 the mother wavelet [15]. To improve estimation performance, it was proposed in [13] to estimate a collection of $M \times M$ multivariate wavelet spectra, computed for non-overlapping windows, $w = 1, \ldots, 2^{j-j_2}$

$$S^{(w)}(2^j) \triangleq \frac{1}{n_{j_2}} \sum_{k=1+(w-1)n_{j_2}}^{wn_{j_2}} D_Y(2^j, k) D_Y(2^j, k)^*. \quad (2)$$

The eigenvalues $\{\lambda_1^{(w)}(2^j), \ldots, \lambda_M^{(w)}(2^j)\}$, computed independently at each scale 2^j and for each window w, are then averaged across windows, after a logarithmic transformation : $\bar{\lambda}_m(2^j) \triangleq 2^{j_2-j} \sum_{w=1}^{2^{j-j_2}} \log_2(\lambda_m^{(w)}(2^j))$. The behaviors along scales 2^j of these averaged log-eigenvalues provide relevant linear regression-based estimation of $\underline{H}$ [13], with v_j classical weights verifying $\sum_j j v_j = 1$ and $\sum_j v_j = 0$ [12]

$$\hat{H}_m = \left(\sum_{j=j_1}^{j_2} v_j \bar{\lambda}_m(2^j) \right) / 2 - \frac{1}{2}, \quad \forall m = 1, \ldots, M. \quad (3)$$

3 Selfsimilarity parameter equality test

Test methodology. Let us assume that, by definition, the vector $\underline{H}$ is sorted, $\forall m = 1, \ldots, M-1, H_{m+1} \geq H_m$. The null hypothesis for a pairwise consecutive selfsimilarity parameter equality tests is defined for each of the $M-1$ consecutive pairs

$$\mathcal{H}_0^{(m)} : H_{m+1} - H_m \equiv 0, \quad m = 1, \ldots, M-1. \quad (4)$$

The test statistics is constructed from the vector of M estimates $\underline{\hat{H}}$ obtained from a single observation of finite-size M-variate data (cf. Eq. 3). Then, $\underline{\hat{H}}$ is sorted in ascending order, $\underline{\hat{H}}_\tau = (\hat{H}_{\tau(1)}, \ldots, \hat{H}_{\tau(M)})$ with $\hat{H}_{\tau(m+1)} \geq \hat{H}_{\tau(m)}$, $m = 1, \ldots, M-1$, and test statistics $\tilde{\delta}_m$ are defined as

$$\tilde{\delta}_m = \hat{H}_{\tau(m+1)} - \hat{H}_{\tau(m)}, \quad m = 1, \ldots, M-1. \quad (5)$$

The practical use of the test thus entails the knowledge of the distribution of $\tilde{\delta}_m$ under $\mathcal{H}_0^{(m)}$.

Properties of the test statistics $\tilde{\delta}_m$. It was shown in [9, 10] that $\underline{\hat{H}}$ is asymptotically unbiased, with components of equal variances, jointly Gaussian and weakly dependent. In a bivariate setting ($M = 2$), this implies that $\tilde{\delta}_1$ follows a folded normal distribution $\mathcal{FN}_{\tilde{\mu}_1,\tilde{\sigma}_1}$ with parameters $\tilde{\mu}_1 = |H_2 - H_1|$ and $\tilde{\sigma}_1 = \sqrt{\sigma^2_{\hat{H}_1} + \sigma^2_{\hat{H}_2}}$. Under $\mathcal{H}_0^{(m)}$, the distribution of $\tilde{\delta}_1$ simplifies to a Half-Normal distribution.

Monte Carlo simulations, conducted on M-fBm, reported in Section 4.2, show that, at least in a multivariate yet low-dimensional setting , i.e., $3 \leq M \ll N$ (with N the sample size), the distributions of $\tilde{\delta}_m$ are well approximated by folded normal distributions $\mathcal{FN}_{\tilde{\mu}_m,\tilde{\sigma}_m}$, and hence, under $\mathcal{H}_0^{(m)}$, by Half-Normal distributions $\mathcal{HN}_{\tilde{\sigma}_m} \equiv \mathcal{FN}_{0,\tilde{\sigma}_m}$.

In principle, this permits the computation of the p-value, p_m, associated with the rejection of $\mathcal{H}_0^{(m)}$. However, in practice, the parameters $\tilde{\sigma}_m$ (and $\tilde{\mu}_m$) are unknown. It is proposed here to perform their estimation from a single observation of data by means of bootstrap techniques [16].

Multivariate time-scale block bootstrap test. Following [12–14], use is made of a multivariate wavelet domain block bootstrap procedure, so as to reproduce the time-scale multivariate cross-dependence structure of multivariate wavelet coefficients $D(2^j, k)$. Practically, overlapping blocks have size L_B in time, and range across all scales and components jointly. For $r = 1, \ldots, R$, bootstrap resamples are drawn with replacement : $D_j^{*(r)} = (D^{*(r)}(2^j, 1), \ldots, D^{*(r)}(2^j, n_j))$.

From each bootstrap sample $D_j^{*(r)}$, estimates $S^{*(r,w)}(2^j)$ and $\hat{H}_m^{*(r)}$ are computed using Eqs. (2-3) and sorted into $\tilde{H}_{\tau^*(r,m)}^{*(r)}$.

Monte Carlo simulations, conducted on M-fBm, reported in Section 4.3, show that the bootstrap test statistics $\tilde{\delta}_m^{*(r)}$ are well approximated by folded normal distributions $\mathcal{FN}_{\tilde{\mu}_m^*,\tilde{\sigma}_m^*}$ and satisfactorily reproduce the test statistics $\tilde{\delta}_m$. Parameters $\tilde{\mu}_m^*$ and $\tilde{\sigma}_m^*$ are estimated from $\tilde{\delta}_m^{*(r)}$ using a classical maximum likelihood estimator. It consists in solving, from independent samples, $\{x_1, \ldots, x_n\}$, the set of coupled equations

$$\sum_{i=1}^{n} \frac{1 - e^{\frac{2\tilde{\mu}x_i}{\tilde{\sigma}^2}}}{1 + e^{\frac{2\tilde{\mu}x_i}{\tilde{\sigma}^2}}} x_i + n\frac{\tilde{\mu}}{2} = 0, \quad \tilde{\sigma}^2 = \frac{1}{n}\sum_{i=1}^{n} x_i^2 - \tilde{\mu}^2. \quad (6)$$

The corresponding p-values associated with the rejection of $\mathcal{H}_0^{(m)}$ can then be computed as (with $F_{\mathcal{FN}}$ the cumulative distribution function of the folded-normal distribution)

$$\tilde{p}_m^* = 1 - F_{\mathcal{FN}\left(0, \frac{\tilde{\delta}_m}{\tilde{\sigma}_m^*}\right)}, \quad (7)$$

together with, for a significance level α, the test decision :

$$d_\alpha^{(m)} = 1 : \quad \tilde{p}_m^* < \alpha \quad (8)$$

Furthermore, and this in another key outcome of the bootstrap procedure constructed here, the power of the test can be estimated also from a single finite-size observation as

$$\pi(\tilde{\mu}_m^*, \tilde{\sigma}_m^*) = 1 - \mathrm{F}_{\mathcal{FN}(\tilde{\mu}_m^*,\tilde{\sigma}_m^*)}(F^{-1}_{\mathcal{FN}(0,\tilde{\sigma}_m^*)}(1-\alpha)). \quad (9)$$

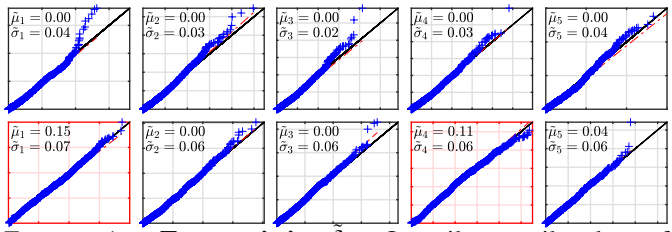

FIGURE 1 – **Test statistics $\tilde{\delta}_m$.** Quantile-quantile plots of $\tilde{\delta}_m$ against samples drawn for a $\mathcal{FN}_{\tilde{\mu}_m,\tilde{\sigma}_m}$, with parameters $\tilde{\mu}_m, \tilde{\sigma}_m$ estimated using Eq. 6, for $m = 1, \ldots, 5$ (from left to right) and Scenario1 (top) and Scenario2 (bottom). Red boxes correspond to departures from $\mathcal{H}_0$ (Scenario2, $m = 1$ and 4).

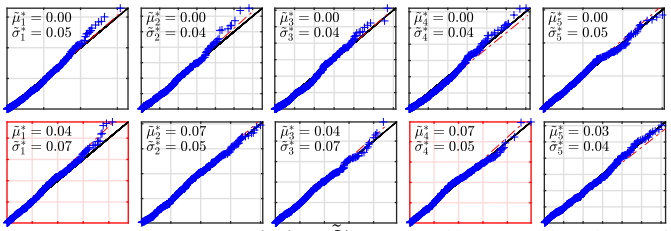

FIGURE 2 – **Test statistics $\tilde{\delta}_m^*$.** Quantile-quantile plots of $\tilde{\delta}_m$ against samples drawn for a $\mathcal{FN}_{\tilde{\mu}_m^*,\tilde{\sigma}_m^*}$, with parameters $\tilde{\mu}_m^*, \tilde{\sigma}_m^*$ estimated using Eq. 6, for $m = 1, \ldots, 5$ (from left to right) and Scenario1 (top) and Scenario2 (bottom). Red boxes correspond to departures from $\mathcal{H}_0$ (Scenario2, $m = 1$ and 4).

4 Monte Carlo Performance Assessment

4.1 Monte Carlo experiment set-up

To assess the relevance of both the folded-normal distribution approximations for the test statistics $\tilde{\delta}_m$ and of the proposed multivariate wavelet domain block bootstrap-based test procedure defined in Section 3, Monte Carlo simulations are conducted, from $N_{MC} = 1000$ independent copies of synthetic $M = 6$-variate M-fBm with sample size $N = 2^{16}$. To validate that the achieved conclusions hold both when all pairs follows $\mathcal{H}_0$ (a single cluster with identical selfsimilarity parameter) and when data comprise different selfsimilarity parameters (several clusters of different sizes), two scenarios are considered :

Scenario1 : A single cluster with $H_1 = \ldots = H_M = 0.8$.

Scenario2 : 3 clusters with different H and sizes (respectively, 1 component with $H_1 = 0.4$, 3 components with $H_2 = 0.6$, and 2 components with $H_3 = 0.8$), such that $\mathcal{H}_0^{(m)}$ is valid for $m = 2, 3, 5$ and not for $m = 1, 4$.

The covariance matrix Σ_X is chosen such that all diagonal entries are set to 1 and all non-diagonal entries are set to $r = 0.5$. The $M \times M$ invertible matrix W is randomly selected and kept fixed for all realizations. Wavelet analysis is performed with the least asymmetric Daubechies3 wavelet. Estimations are performed by linear regressions across scales $2^{j_1} = 2^8$ to $2^{j_2} = 2^{11}$. $R = 500$ block-bootstrap resamples are drawn from overlapping blocks of size $L_B = 6$ (corresponding to the size of the Daubechies3 mother wavelet time support).

4.2 Test statistics properties

Let us start by studying the test statistics $\tilde{\delta}_m$. Fig. 1 reports, for Scenario1 and 2, and for the five pairs $m = 1, \ldots, M - 1$, quantile-quantile plots for the distributions of $\tilde{\delta}_m$ against samples drawn from a folded normal distribution $\mathcal{FN}_{\tilde{\mu}_m,\tilde{\sigma}_m}$, with parameters $\tilde{\mu}_m, \tilde{\sigma}_m$ estimated using Eq. 6.

Fig. 1 shows first that folded normal distributions are relevant approximations for $\tilde{\delta}_m$ under both $\mathcal{H}_0$ and alternative hypothesis $\mathcal{H}_A$, and second that under $\mathcal{H}_0$, $\tilde{\mu}_m \simeq 0$ validating the approximation by the Half-Normal distribution. These Monte Carlo simulations show that, under Scenario1, despite the fact that all pairs follow $\mathcal{H}_0$, it can be observed that, while $\tilde{\mu}_m \simeq 0$ $\forall m$, $\tilde{\sigma}_m$ depend on m : It is larger for $m = 1$ and $m = 5$, i.e., for the smallest and largest estimates $\hat{H}_m$, and smaller for the central estimates, which can be interpreted as a consequence of the sorting operation applied to the elements of $\underline{\hat{H}}$. They also show that, under $\mathcal{H}_0$, the values for $\tilde{\sigma}_m$ for a same m (i.e., $m = 2, 3$ or 5) differ between Scenario1 and Scenario2. These observations constitute the first main and interesting findings : The distribution of $\tilde{\delta}_m$ under $\mathcal{H}_0$ depends both on the rank of the sorted pairs (i.e., on m) and on the scenario, mostly via $\tilde{\sigma}_m$.

4.3 Boostrapped test statistics properties

Folded-normal modeling. Let us now turn to the bootstrap test statistics $\tilde{\delta}_m^*$. Fig. 2 reports, for Scenario1 and 2, and for the five pairs $m = 1, \ldots, M - 1$, quantile-quantile plots for the distributions of $\tilde{\delta}_m^*$ against samples drawn from $\mathcal{FN}_{\tilde{\mu}_m^*,\tilde{\sigma}_m^*}$, with $\tilde{\mu}_m^*, \tilde{\sigma}_m^*$ estimated using Eq. 6. Fig. 2 shows that $\tilde{\delta}_m^*$ are well approximated by folded-normal distributions under both $\mathcal{H}_0$ and $\mathcal{H}_A$ and for both scenarios.

Bootstrap parameter estimation. Table 1 shows that the estimates of $\tilde{\mu}_m^*$ and $\tilde{\sigma}_m^*$ averaged across Monte Carlo simulations compare well to $\tilde{\mu}_m, \tilde{\sigma}_m$, thus validating that the bootstrap test statistics $\tilde{\delta}_m^*$ satisfactorily reproduce the test statistics $\tilde{\delta}_m$.

TABLE 1 – Folded-Normal parameter estimates (Monte Carlo average $\pm$ 95% confidence intervals). Red boxes correspond to departures from $\mathcal{H}_0$ (Scenario2, $m = 1$ and 4).

$\times 10^2$		$m = 1$	$m = 2$	$m = 3$	$m = 4$	$m = 5$
Scenario1	$\tilde{\mu}_m$	0.0	0.0	0.0	0.0	0.0
	$\tilde{\sigma}_m$	4.3	2.8	2.5	2.8	3.9
	$\tilde{\mu}_m^*$	0.9 ± 0.2	0.1 ± 0.0	0.1 ± 0.0	0.1 ± 0.0	0.6 ± 0.1
	$\tilde{\sigma}_m^*$	5.7 ± 0.1	3.9 ± 0.1	3.4 ± 0.0	3.6 ± 0.0	4.6 ± 0.1
Scenario2	$\tilde{\mu}_m$	14.7	0.0	0.0	11.0	3.7
	$\tilde{\sigma}_m$	7.3	5.9	5.7	6.1	5.8
	$\tilde{\mu}_m^*$	14.4 ± 0.5	3.0 ± 0.2	2.7 ± 0.2	10.4 ± 0.3	5.3 ± 0.2
	$\tilde{\sigma}_m^*$	7.4 ± 0.1	6.3 ± 0.1	5.9 ± 0.1	5.8 ± 0.0	6.1 ± 0.1

Bootstrap test p-values. Further, Fig. 3 shows that the bootstrap-based estimates of the test p-value $\tilde{p}_m^*$ (computed from Eq. 7) approximately follow a uniform distribution under $\mathcal{H}_0$. As expected, these $\tilde{p}_m^*$ depart from a uniform distribution under $\mathcal{H}_A$.

Bootstrap test performance. Finally, Table 2 compares, for a preset significance level $\alpha = 0.05$, averages across Monte Carlo realizations of the test decisions $d_\alpha^{(m)}$ (i.e., percentage

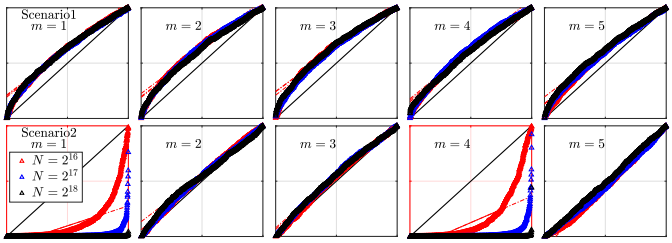

FIGURE 3 – **Bootstrap estimates of the test p-values.** Quantile-quantile plots of $\tilde{p}^*_m$ (computed from Eq. 7) against samples drawn from a uniform distribution, for several sample sizes N Red boxes correspond to departures from $\mathcal{H}_0$ (Scenario2, $m = 1$ and $m = 4$).

TABLE 2 – Bootstrap estimate of the test power $\pi(\tilde{\mu}^*_m, \tilde{\sigma}^*_m)$ (cf. Eq 9). Red boxes indicates departures from $\mathcal{H}_0$.

	N		$m=1$	$m=2$	$m=3$	$m=4$	$m=5$
Scenario1	2^{16}	$\langle d_\alpha^{(m)} \rangle$	0.02	0.01	0.02	0.01	0.02
		$\pi(\tilde{\mu}^*_m, \tilde{\sigma}^*_m)$	0.07	0.05	0.05	0.05	0.06
	2^{17}	$\langle d_\alpha^{(m)} \rangle$	0.01	0.01	0.01	0.01	0.01
		$\pi(\tilde{\mu}^*_m, \tilde{\sigma}^*_m)$	0.06	0.05	0.05	0.05	0.06
	2^{18}	$\langle d_\alpha^{(m)} \rangle$	0.01	0.01	0.00	0.00	0.01
		$\pi(\tilde{\mu}^*_m, \tilde{\sigma}^*_m)$	0.06	0.05	0.05	0.05	0.06
Scenario2	2^{16}	$\langle d_\alpha^{(m)} \rangle$	0.51	0.05	0.05	0.49	0.09
		$\pi(\tilde{\mu}^*_m, \tilde{\sigma}^*_m)$	0.51	0.11	0.11	0.46	0.19
	2^{17}	$\langle d_\alpha^{(m)} \rangle$	0.92	0.04	0.04	0.89	0.07
		$\pi(\tilde{\mu}^*_m, \tilde{\sigma}^*_m)$	0.83	0.12	0.11	0.76	0.18
	2^{18}	$\langle d_\alpha^{(m)} \rangle$	1.00	0.03	0.04	1.00	0.06
		$\pi(\tilde{\mu}^*_m, \tilde{\sigma}^*_m)$	0.99	0.11	0.11	0.97	0.18

of rejections $d_\alpha^{(m)} = 1$) and of the test powers, $\pi(\tilde{\mu}^*_m, \tilde{\sigma}^*_m)$, computed from Eq. 9. The results indicate that i) the test closely reproduces the preset false alarm rate α under $\mathcal{H}_0$, ii) has reasonable power under $\mathcal{H}_A$ and iii) the estimate $\pi(\tilde{\mu}^*_m, \tilde{\sigma}^*_m)$ satisfactorily reproduce the percentage of rejections under both scenarios and under both $\mathcal{H}_0$ and $\mathcal{H}_A$.

5 Conclusions and perpectives

A multivariate wavelet-domain block bootstrap procedure was constructed to test pairwise equality of selfsimilarity parameters in multivariate selfsimilar data from a single finite-size observation. The bootstrap test statistic was shown to well reproduce the distribution of the actual pairwise test statistic both when all H are equal and when there exist clusters of different sizes with different values of Hs, a non trivial result. The bootstrap procedure was also shown to well estimate the power of the test, another interesting outcome. Further, the procedure was shown to have a large power for large size data, that however drops fast when sample size decreases. Future work will include investigating different scenarios and whether alternative (here, consecutive comparisons of sorted estimates of $\underline{H}$), robust to lower sample sizes, strategies can be constructed.

References

[1] P. Abry, H. Wendt, S. Jaffard, and G. Didier, "Multivariate scale-free temporal dynamics : From spectral (fourier) to fractal (wavelet) analysis," *Comptes Rendus Physique*, vol. 20, no. 5, pp. 489–501, 2019.

[2] B. B. Mandelbrot and J. W. van Ness, "Fractional Brownian motion, fractional noises and applications," *SIAM Reviews*, vol. 10, pp. 422–437, 1968.

[3] G. Samorodnitsky and M. Taqqu, *Stable non-Gaussian random processes*, Chapman and Hall, New York, 1994.

[4] V. Pipiras and M. S. Taqqu, *Long-Range Dependence and Self-Similarity*, vol. 45, Cambridge Univ. Press, 2017.

[5] M. Maejima and J. D. Mason, "Operator-self-similar stable processes," *Stochastic Processes and their Applications*, vol. 54, no. 1, pp. 139–163, 1994.

[6] J. D. Mason and Y. Xiao, "Sample path properties of operator-self-similar Gaussian random fields," *Theory of Proba. & Its Applications*, vol. 46, no. 1, pp. 58–78, 2002.

[7] G. Didier and V. Pipiras, "Integral representations and properties of operator fractional Brownian motions," *Bernoulli*, vol. 17, no. 1, pp. 1–33, 2011.

[8] P.-O. Amblard and J.-F. Coeurjolly, "Identification of the multivariate fractional brownian motion," *IEEE Transactions on Signal Processing*, vol. 59, no. 11, pp. 5152–5168, 2011.

[9] P. Abry and G. Didier, "Wavelet estimation for operator fractional Brownian motion," *Bernoulli*, vol. 24, no. 2, pp. 895–928, 2018.

[10] P. Abry and G. Didier, "Wavelet eigenvalue regression for n-variate operator fractional Brownian motion," *Journal of Multivariate Analysis*, vol. 168, pp. 75–104, 2018.

[11] D. La Rocca, H. Wendt, V. Van Wassenhove, Ph. Ciuciu, and P. Abry, "Revisiting functional connectivity for infraslow scale-free brain dynamics using complex wavelets," *Frontiers in Physiology*, p. 1651, 2021.

[12] H. Wendt, P. Abry, and G. Didier, "Wavelet domain bootstrap for testing the equality of bivariate self-similarity exponents," in *Proc. IEEE Workshop Statistical Signal Proces. (SSP)*, Germany, 2018.

[13] C.-G. Lucas, P. Abry, H. Wendt, and G. Didier, "Bootstrap for testing the equality of selfsimilarity exponents across multivariate time series," in *Proc. European Signal Processing Conference (EUSIPCO)*, Ireland, 2021.

[14] C.-G. Lucas, P. Abry, H. Wendt, and G. Didier, "Counting the number of different scaling exponents in multivariate scale-free dynamics : Clustering by bootstap in the wavelet domain," in *International Conference on Acoustics, Speech, and Signal Processing (ICASSP)*, 2022.

[15] S. Mallat, *A Wavelet Tour of Signal Processing*, Academic Press, San Diego, CA, 1998.

[16] A. M. Zoubir and D. R. Iskander, *Bootstrap techniques for signal processing*, Cambridge University Press, 2004.